DEMONSTRATION OF PSEUDO-DUCTILITY IN QUASI-ISOTROPIC LAMINATES COMPRISING THIN-PLY UD CARBON/EPOXY HYBRID SUB-LAMINATES

G. Czél[1*,2], T. Rév[2], M. Jalalvand[2], M. Fotouhi[2], M. R. Wisnom[2]

[1]MTA–BME Research Group for Composite Science and Technology, Budapest University of Technology and Economics, Műegyetem rkp. 3., H-1111 Budapest, Hungary
*Email: czel@pt.bme.hu, Web Page: http://www.pt.bme.hu
[2]Advanced Composites Centre for Innovation and Science (ACCIS), University of Bristol, Queens Building, University Walk, Bristol BS8 1TR, United Kingdom
Web Page: http://www.bristol.ac.uk/composites/

Keywords: Pseudo-ductility, quasi-isotropic, carbon/epoxy

Abstract
Un-notched and notched tensile response and damage accumulation of quasi-isotropic carbon/epoxy hybrid laminates were studied. It was confirmed that ply fragmentation demonstrated previously as a successful ductility mechanism can be stransferred to multi-directional laminates. Furthermore, notch-insensitivity was demonstrated by locally active fragmentation in a notched quasi-isotropic laminate.

1. Introduction

High performance polymer matrix composites are suitable for high-tech applications such as military and civil aerospace, spacecraft or motorsports due to their outstanding specific stiffness and strength, fatigue and corrosion resistance. However, a fundamental limitation of current fibre reinforced composites is their inherent brittleness which has hindered their spread towards many high volume applications. Failure of composites can be sudden and catastrophic, with little or no warning and usually poor residual load-carrying capacity if any. High performance composites showing progressive damage and gradual failure similar to that of ductile metals are of significant interest and could extend the scope of applications towards new fields such as automotive or construction.
The authors presented favourable pseudo-ductile failure in uni-directional (UD) glass/carbon [1],[2], and carbon/carbon [3] fibre hybrid composites recently. Based on the favourable properties of UD hybrids such as progressive damage through fragmentation and stable delamination of the central low strain layer from the outer high strain layers and a wide safety margin between damage initiation and final failure, the aim of the present work is to demonstrate pseudo-ductility in multi-directional laminates which are suitable for a wide variety of structural applications. The approach to be presented is the use of interlayer hybrid sub-laminates of different grade carbon fibre/epoxy prepregs as building blocks for a quasi-isotropic (QI) plate.

2. Experimental

2.1. Specimen design and geometry

Figure 1. shows the hybrid sub-laminate concept applied to build up a QI laminate of UD building blocks. The main design considerations for the QI laminates were the following: (i) the sub-laminate should fail stably with no delamination, (ii) the thickness of the sub-laminate should be kept low, to

hinder free-edge delamination, (iii) avoid double 90° layers in the middle of the laminate to suppress transverse cracking and induced delamination.

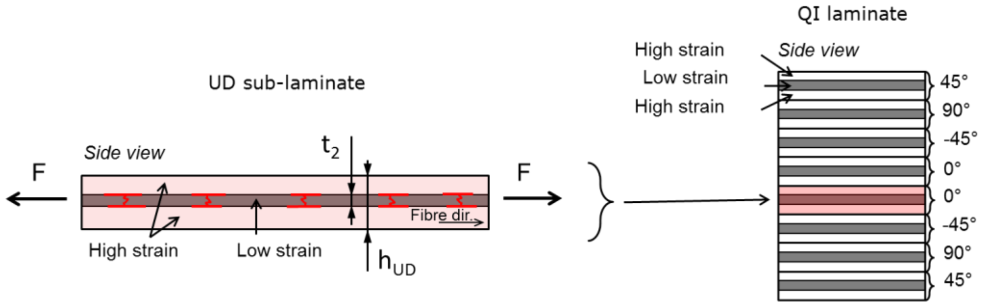

Figure 1. Sub-laminate concept for QI hybrid laminates

Figure 2. highlights the 2 levels of delamination considered in the design phase. Both figures show the designed orientations of the sub-laminates in the QI laminate which is $[45/90/\text{-}45/0]_s$. The blocked 0° sub-laminates were put in the middle to avoid early extensive delamination which could have started from the matrix cracking of blocked 90° sub-laminates.

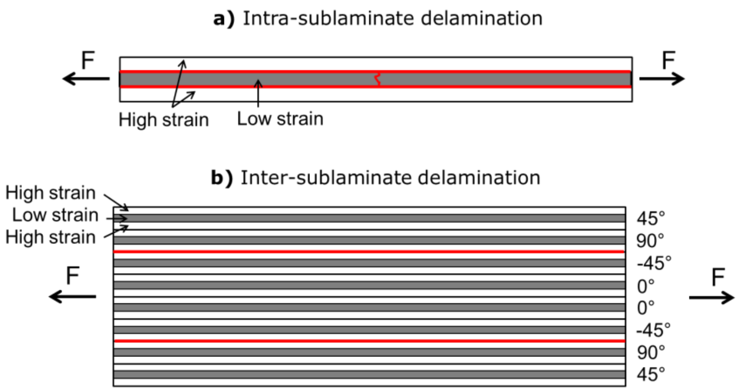

Figure 2. Sub-laminate concept for QI hybrid laminates

Figure 3. shows the geometric parameters on the side and top view schematics of a QI hybrid composite tensile specimen. Nominal specimen dimensions were 120/64/16/h mm-overall length/ free length (L_f)/ width (W)/ variable thickness (h) respectively (except for the UD sub-laminate configuration where 240/160/20/h mm size specimens were tested (see Table 4.)).

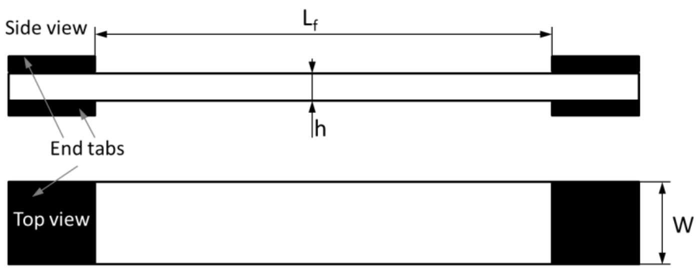

Figure 3. Specimen schematic

2.2. Materials

The materials considered for design, and used in the experimental part of the study were T1000 and XN80 carbon/epoxy prepregs from North Thin-Ply Technology. The resin type in the prepregs was

North's ThinPreg 120 EPHTg- 402 type 120°C cure, medium viscosity, toughened epoxy system. Properties of the utilised fibres and prepreg systems can be found in table 1. and table 2.

Table 1. Fibre properties of the applied UD prepregs based on manufacturer's data

Fibre type	Manufacturer	Elastic modulus [GPa]	Strain to failure [%]	Tensile strength [GPa]	Density [kg/m^3]
Torayca T1000	**Toray**	294	2.2	6.37	1800
Granoc XN80	**Nippon GFC**	780	0.5	3.43	2170

Table 2. Material properties of the cured UD prepreg composites utilised. (All figures were calculated from manufacturer's data.)

Prepreg material	Manufacturer	Fiber mass per unit area [g/m^2]	Cured ply thickness [μm]	Fibre volume fraction [%]	Initial elastic modulus [GPa]
T1000/epoxy	North TPT	28	32.4	48.1	143
XN80/epoxy	North TPT	63	62.3	46.5	365

2.3. Manufacturing

UD three layer hybrid sub-laminates of T1000/epoxy as the high and XN80/epoxy as the low strain materials respectively (see Fig. 1.) were prepared first using individual plies cut out from the prepreg rolls according to the future orientation of the given sub-laminate in the QI plate. These prepared building blocks were then stacked together by aligning the straight edges of the sub-laminates and keeping the pre-defined orientations to build the QI hybrid laminate. Both applied prepregs had a common 120ºC cure epoxy resin system and were cured in an autoclave according to the manufacturer's recommendation: 2 hours@120ºC, 0.7 MPa.

2.4. Test procedure

Un-notched and notched tensile testing of the hybrid composite specimens was executed under uniaxial tensile loading and displacement control using a crosshead speed of 1 and 0.5 mm/min for un-notched and notched specimens respectively on a computer controlled Instron 8801 type 100 kN rated universal hydraulic test machine with wedge type hydraulic grips. Relative extensions were measured using an Imetrum videogauge system with a nominal gauge length 10 mm shorter than the free length of the specimens. The measured relative extensions therefore include the full width and the notched parts of the specimens where relevant. The obtained relative extensions correspond to the surface of the specimens and their accuracy is affected by local and/or global delamination and/or splitting of the surface plies after the first occurrence of any of these damage events. Overall videos recorded by the videogauge camera were also kept to be used for failure type and sequence characterisation.

2.5. Specimen types

The tested specimen configurations are given in Table 3. The calculated energy release rates for the UD sub-laminates based on equation (1) are included in the table because it is an important parameter determining the stability of delamination between the low and high strain layers within the hybrid sub-laminates at low strain material fracture. The details of the fracture mechanics calculations yielding equation (1) can be found in [1].

$$G_{II} = \frac{\varepsilon^2 E_2 t_2 \left(E_1 (h - t_2) + E_2 t_2\right)}{4 E_1 (h - t_2)} \tag{1}$$

where G_{II} is the mode II energy release rate of the specimen ε is the overall strain in the hybrid composite, E_1 is the modulus of elasticity of the low strain material (LSM), E_2 is the modulus of elasticity of the high strain material (HSM), h_{UD} is the overall thickness of the hybrid sub-laminate, t_2 is the thickness of the low strain layer (see Fig. 1.).

Table 3. Properties of the configuration designed and tested within the present study

Specimen type	**Areal mass** [g/m^2]	**Nominal thickness** [mm]	**Relative LSM thickness (to full)** [-]	**Predicted intra-sub-laminate G_{II} at LSM failure strain** [N/mm]	**Predicted inter-sub-laminate G at LSM failure strain** [N/mm]
[$T1000_2$/$XN80_1$/$T1000_2$]	56/63/56	0.192	0.325	0.317	0.146

The low intra-sublaminate energy release rate in Table 3. suggest, that the designed sub-laminates will provide fragmentation and stable delamination within the 0° direction sub-laminates as previous tests of similar materials indicated that the mode II fracture toughness of the North TPT prepregs is around G_{IIC}=0.5 N/mm. The inter-sublaminate energy release rate for delmaination between the hybrid sub-laminates with different fibre orientation is calculated at the failure strain of the low strain material of the hybrid sub-laminate using the analytical method suggested by O'Brien **Error! Reference source not found.** and shown in Table 3. This is a good analytical approximating method based on the stiffness reduction after delamination and it includes a few assumptions such as two symmetric delaminations against the mid-plane which is likely fulfilled in the tested laminates. The outcome of this method is the total energy release rate so it should be compared against mixed-mode critical energy release rate. The calculated G=0.146 N/mm at XN80 failure is significantly lower than either the typical mode I or II fracture toughness composite interfaces (0.2 and 1 N/mm respectively) therefore free edge delamination is expected to be suppressed in the designed QI hybrid laminate at least until the start of fragmentation.

Two different notches were applied for the QI hybrid specimens: (i) open hole with a 3.175 mm diameter (1/5 of the specimen width), and (ii) 3.2 mm long (1/5 of the specimen width) sharp notch machined with a 2 mm diameter ball end mill and sharpened manually with an 180 µm wide diamond wire saw. Un-notched tensile tests of the UD sub-laminate were also executed to have an understanding of how can the pseudo-ductility of the sub-laminates be translated to the laminate response. Table 4. shows the number of specimens tested from each type.

Table 4. Types and number of tested specimens of each type

Number of specimens tested	**UD sub-laminate (UD)**	**QI un-notched (UN)**	**QI open-hole (OH)**	**QI sharp-notched (SN)**
T1000/XN80	6	6	6	6

2.6. Results and discussion

Fig. 4. shows the favourable pseudo-ductile tensile behaviour of the UD hybrid sub-laminate made of T1000 and XN80 fibres. The high stiffness, low strain XN80 fibres started to fragment around 0.5% strain at the so-called pseudo-yield point. This is the beginning of a stable, progressive damage process along the approximately 0.4% wide strain plateau when fragmentation and stable delamination around the cracks in the XN80 plies took place. After the high (over 1000 MPa) stress plateau the stress started to rise again as the T1000 plies took more load upon saturation of fragmentation. The significant (up to 1%) so-called pseudo-ductile strain between damage initiation and final failure

shows potential to address the brittle failure of the QI laminate as well. The observed failure type agrees well with that expected according to the design considerations.

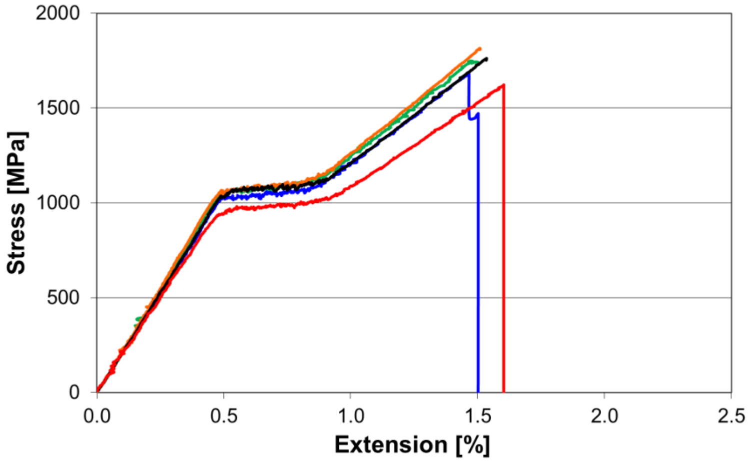

Figure 4. Tensile response of the UD sub-laminate specimens

Fig. 5. shows the tensile response of the QI un-notched T1000/XN80 hybrids. It is obvious from the graphs that the fragmentation in the 0° sub-laminates started at about a 0.3% lower strain than the first load drops corresponding to inter-sub-laminate delaminations. It is worth noting, that the start of the plateau was shifted from 0.49% (UD) to approximately 0.59% (QI) which is probably due to the contribution of the off-axis sub-laminates to the load bearing in the thicker QI laminate which masked the loss of stiffness visible on the graphs as a slight decrease in slope from about 0.4% strain in the initial phase of fragmentation. The off-axis plies may have slightly delayed the extensive fragmentation stage as well required to start the stress plateau. The obvious stable plateau before the first load drops confirms that both key pseudo-ductility mechanisms of thin-ply UD hybrids (i.e. fragmentation and stable intra-sub-laminate pull-out in the 0° direction) were successfully transferred into QI laminates and delamination was suppressed until about 0.85% strain.

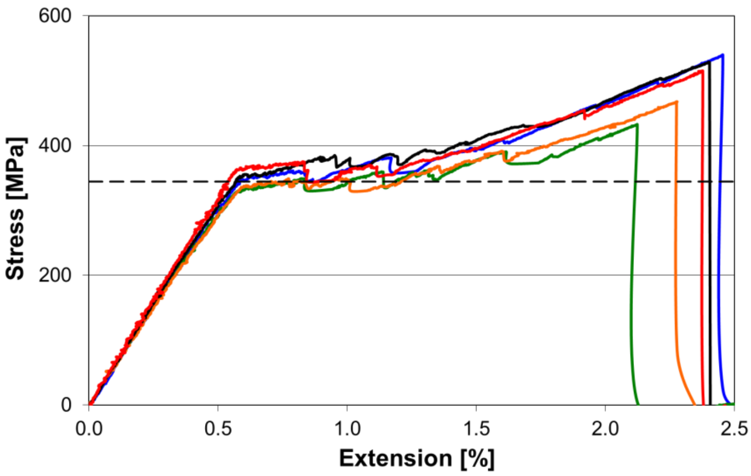

Figure 5. Tensile response of the un-notched QI specimens

Fig. 6. shows the net section tensile response of the open-hole QI T1000/XN80 specimens calculated to a cross section excluding the notch. The figure reveals that the damage initiated only at a slightly lower overall extension than in the un-notched case and the stress for the first load-drop was higher than the pseudo-yield stress of the un-notched specimens indicated by the dashed line on Fig.5. The

test curves show significant deviations from the initial straight line before the first load drop, which indicates local damage around the hole before the first load drop corresponding to extensive delamination.

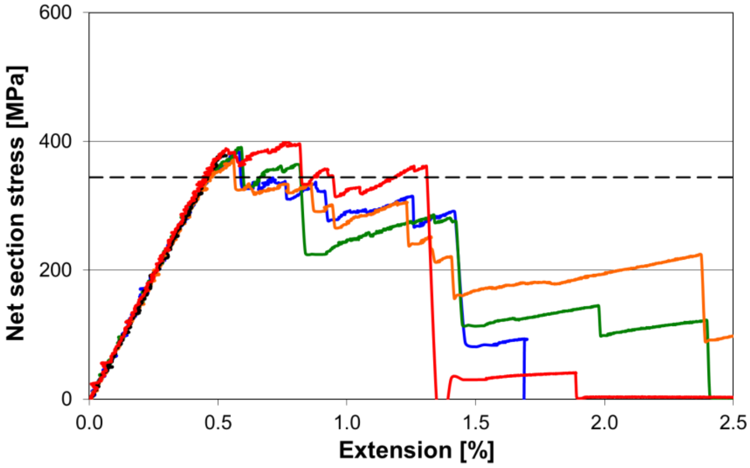

Figure 6. Tensile response of the open-hole QI specimens

Fig. 7. shows the net section tensile response of the sharp-notched QI T1000/XN80 specimens. The behaviour was very similar to that of the open-hole specimens probably because fibre reinforced composites are not so sensitive to the shape of the discontinuity across the specimen width as similarly brittle, but homogeneous materials. Small non-linear sections were observed for this notch geometry as well in the stress-strain responses before the first load-drops and the stress at the first load-drop was significantly higher than the pseudo-yield stress of the un-notched specimens. The overall shape of the curves reveals that large load-drops took place earlier in the sharp-notched specimens than in the open-hole ones which indicates slightly different delamination mechanisms.

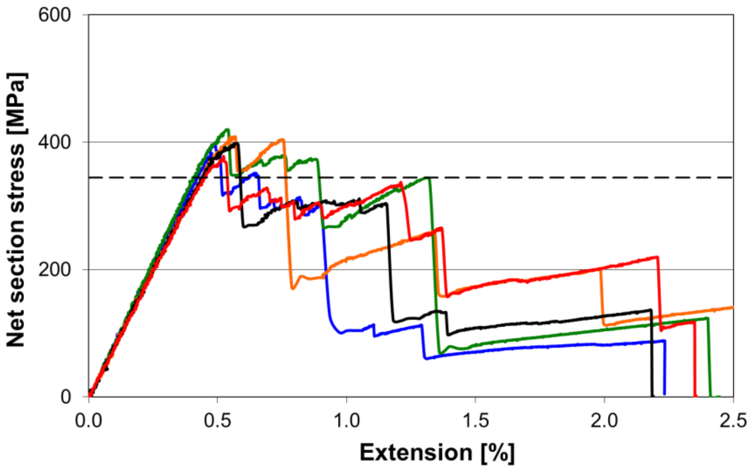

Figure 7. Tensile response of the sharp notched QI specimens

Table 5. summarises the results of the tested specimen types. It is interesting to note, that the onset of damage was about 0.1% lower for the QI notched specimens than for the QI un-notched ones. This indicates that the LSM fragmentation cannot result in a significant change in stiffness until a point well beyond damage initiation in un-notched QI laminates. A detectable (0.08-0.11%) strain margin was observed between the onset of damage and the first load drop due to delamination in the notched QI specimen types which corresponded to local pseudo-ductile damage around the notches. It was also noted, that the notched net section strength of the specimens (see dashed lines on the graphs) was

higher than the pseudo-yield stress of the un-notched specimens, which can be interpreted as notch-insensitivity.

Table 5. Summary of test results (Specimen types: UD- uni-directional, UN- un-notched, OH- open-hole, SN- sharp-notched)

Spec. type	Nominal thickness	Nominal width	Nominal free length	Notch size	Measured modulus from nominal thickness	Damage onset strain	Pseudo-yield/ plateau stress	Final failure strain	Maximum (net section) stress
	[mm]	[mm]	[mm]	[mm] (CV%)	[GPa] (CV%)	[%] (CV rel.%)	[MPa] (CV%)	[%] (CV rel.%)	[%] (CV rel.%)
T1000/XN80-UD	0.192	20	160	-	207.9 (3.0)	0.49[1] (1.8)	1030.3 (3.9)	-	-
T1000/XN80-UN	1.54	16	64	-	62.2 (2.4)	0.55[2] (2.8)	344.4[2] (4.2)	-	497 (9.1)
T1000/XN80-OH	1.54	16	64	3.2	62.3 (1.1)	0.457[3] (5.5)	-	0.568 (3.9)	385.3 (2.4)
T1000/XN80-SN	1.54	16	64	3.47 (7.6)	64.9 (2.5)	0.449[3] (2.6)	-	0.534 (5.8)	399.5 (4.1)

[1]Recorded at first small load drop
[2]Recorded at the intersection of lines fitted to the linear and the plateau part of the stress-strain curves
[3]Recorded at the onset of non-linearity using the intersection of fitted lines

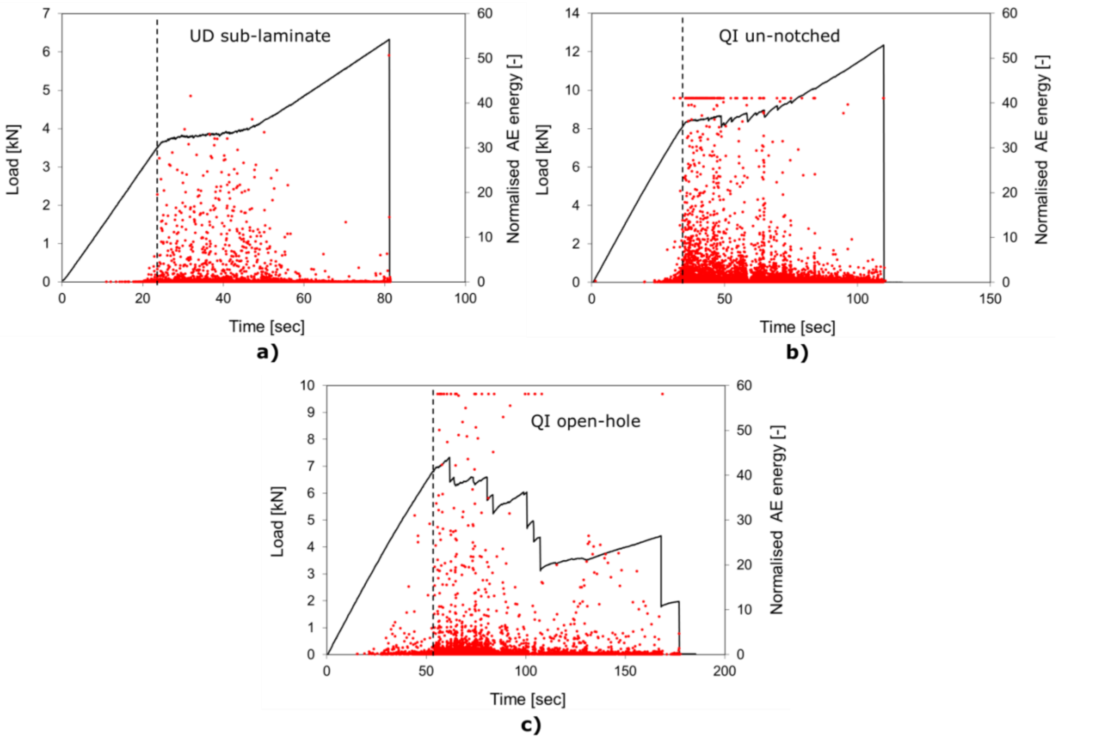

Figure 8. Graphs showing the acoustic event energy normalised to the average for a typical one of the a) UD sub-laminate, b) QI un-notched and c) QI sharp notched specimen configurations. Dashed lines correspond to the damage initiation.

2.7. Acoustic emission (AE) damage analysis

The accumulation of damage was monitored in a few specimens of each configurations with a PAC PCI-2 type acoustic emission device at a 5 MHz sampling rate using two WSA type 100-1000 kHz wideband sensors attached to the specimens with clips and silicone grease as an acoustic coupler. The scope of these measurements was to study the damage initiation in the different specimen configurations by detecting low strain ply fragmentation in the 0° sub-laminates [4]. Fig. 8. shows typical plots of the acoustic energy normalisedto the average event energy for three different configurations. The vertical dashed lines show the fragmentation initiation estimated from the AE signs. Part a) and b) reveals very low acoustic activity before the pseudo-yield point, for the sub-laminate and the QI un-notched configuration and very strong activity during the plateau. This demonstrates that the ply fragmentation mechanism can be exploited for pseudo-ductility in multi-directional laminates. Interestingly, part c) indicates that high energy events were released significantly earlier than the first load drop in the QI open hole specimens, which means that local fragmentation took place at the notch before the first delamination. The decreased short, slope section of the load curve before the first load drop is the counterpart of the stress plateau in the un-notched configuration but in this case the plateau only develops in the volume local to the notch. Since the mechanical test curves only indicate the overall time-load relation of the whole gauge length, the fragmentation mechanism being active only locally at the notch is masked. The dense pattern of high energy acoustic events confirms that fragmentation is active during this masked plateau before the first delamination. This key finding demonstrates that the fragmentation mechanism can be active locally at a notch tip and re-distribute loads thereby improving notch sensitivity.

3. Conclusions

The following conclusions were drawn from the study of thin-ply carbon/epoxy hybrid laminates:

- The tested un-notched QI T1000/XN80 type specimens showed gradual failure and demonstrated a stress plateau before the first delamination induced load-drops, followed by a significant stress peak before final failure. These features can be exploited for warning and safety margin in structural applications.
- The tested QI laminate showed pseudo-ductile features i.e. stress plateaus in their un-notched stress-strain responses demonstrating the successful transfer of the ductility mechanisms (i.e. low strain material fragmentation and stable pull-out) which were exploited previously only in UD hybrids into multi-directional hybrid compostes.
- The notched strength of the QI specimens was higher than the pseudo-yield stress of the corresponding un-notched specimens regardless of the notch shape (i.e. hole or sharp). This demonstrates notch-insensitivity.
- The acoustic emission damage study indicated that fragmentation took place locally in the notched specimens and allowed for redistribution of the loads resulting in favourable response.

Acknowledgments

This work was funded under the UK Engineering and Physical Sciences Research Council Programme Grant EP/I02946X/1 on High Performance Ductile Composite Technology in collaboration with Imperial College, London. Gergely Czél acknowledges the Hungarian Academy of Sciences for funding through the Post-Doctoral Researcher Programme fellowship scheme, the János Bolyai scholarship and the Hungarian National Research, Development and Innovation Office - NKFIH, for funding through grant OTKA K 116070. Data can be requested from the corresponding author.

References

[1] G. Czél and M.R. Wisnom. Demonstration of pseudo-ductility in high performance glass-epoxy composites by hybridisation with thin-ply carbon prepreg. *Composites Part A: Applied Science and Manufacturing*, 52:23–30, 2013.

[2] G. Czél, M. Jalalvand and M.R.Wisnom. Design and characterisation of advanced pseudo-ductile unidirectional thin-ply carbon/epoxy-glass/epoxy hybrid composites. *Composite Structures*, 143:362-370, 2016.

[3] G. Czél, M. Jalalvand and M.R.Wisnom. Pseudo-ductile carbon/epoxy hybrid composites. *Proceedings of the 20th International Conference on Composite Materials ICCM-20, Copenhagen, Denmark*, July 19-24 2015.

[4] M Fotouhi, P Suwarta, M Jalalvand, G Czel, MR Wisnom. Detection of fibre fracture and ply fragmentation in thin-ply UD carbon/glass hybrid laminates using acoustic emission, *Composites Part A: Applied Science and Manufacturing*, 86:66–76, 2016.